

Background dynamics and observational constraints of flat and non-flat $\Lambda(t)$ CDM models from $H(z)$ and DESI DR2 BAO measurements

Olga Avsajanishvili¹

¹*Evgeni Kharadze Georgian National Astrophysical Observatory, Tbilisi 0179, Georgia*

(Dated: March 5, 2026)

In this work, we present comprehensive observational constraints on the time-varying vacuum $\Lambda(t)$ CDM cosmology using the latest baryon acoustic oscillation (BAO) data from Dark Energy Spectroscopic Instrument (DESI) Data Release 2 measurements in combination with cosmic chronometer $H(z)$ data. We explicitly quantify the impact of vacuum dynamics on the expansion history, the total effective equation of state parameter of the unified cosmic fluid, the effective dark energy equation of state parameter, and the deceleration parameter in the spatially flat $\Lambda(t)$ CDM model. We perform a full Markov Chain Monte Carlo (MCMC) analysis and statistical model comparison, providing a consistent assessment of the $\Lambda(t)$ CDM model relative to the standard Λ CDM framework. Our results demonstrate that $H(z)$ and BAO observations strongly constrain deviations from the Λ CDM model, driving the vacuum dynamics parameter toward $\alpha \simeq 0$, while significantly reducing parameter degeneracies and alleviating the Hubble tension.

I. INTRODUCTION

The standard spatially flat cosmological Lambda Cold Dark Matter (Λ CDM) model [1–3] has demonstrated good consistency with a wide range of observational probes accumulated over the last several decades [4–7]. Nevertheless, despite its status as the current concordance model, the Λ CDM model exhibits a number of statistically significant tensions and anomalies [8–12]. Among the various discrepancies reported in the literature, one of the most prominent is the tension in the Hubble constant H_0 , manifested as a statistically significant disagreement between the value inferred from Planck Cosmic Microwave Background (CMB) observations [5] and that obtained from local distance-ladder measurements by Supernova H_0 for the Equation of State (SH0ES) collaboration [13]. In this context, another long-standing open issue in modern cosmology is the so-called coincidence problem, namely, the question of why the energy densities of dark energy (DE) and dark matter (DM) are of the same order of magnitude precisely at the present cosmic epoch [14–21].

The interacting DE (IDE) models [22–26] address this problem by allowing energy exchange between DE and DM, effectively allowing dynamical interplay between these two components [22–26]. Such interactions can naturally modify the late-time expansion history of the universe, providing a viable mechanism to alleviate the coincidence problem and, through the resulting changes in the background dynamics, offering a phenomenological avenue to ease the observed H_0 tension [27–37].

The time-varying Lambda Cold Dark Matter ($\Lambda(t)$ CDM) model [31, 38–45] belongs to a wide class of IDE scenarios. This model represents a phenomenological extension of the standard Λ CDM cosmology in which the vacuum energy density is allowed to evolve with cosmic time and interact with the matter sector. The interaction between matter and vacuum energy is parametrized by a single dimensionless vacuum dynam-

ics parameter α ¹, which quantifies departures from the standard Λ CDM model and ensures a continuous Λ CDM limit for $\alpha = 0$, fully recovered only asymptotically in the future.

At the background level, this model can be interpreted as equivalent to a Generalized Chaplygin Gas (GCG), providing a phenomenological unified description of DM and DE as a single fluid. The concept of unifying DM and DE was first introduced by Chaplygin [55], and the original Chaplygin model, along with its various generalizations, has been extensively studied both theoretically and observationally [56–72]. The GCG arises from a barotropic fluid with the equation of state (EoS) $p = -A/\rho^\alpha$, where p and ρ are the pressure and the energy density of the barotropic fluid, respectively; $A > 0$ is a constant and α is the model parameter (typically $\alpha > -1$ to avoid singularities)². It was originally proposed to account for the observed cosmic acceleration without invoking separate DM and DE components [64, 73–82]. In this framework, the unified fluid behaves like DM during the early stages of cosmic evolution and asymptotically approaches a cosmological constant at late times, with vacuum energy interacting with matter.

In this work, we reconstruct the total effective EoS

¹ The $\Lambda(t)$ CDM model is closely related to the running vacuum model (RVM) [46–54], as both scenarios belong to the class of cosmologies with dynamical vacuum energy interacting with matter. While RVM is typically formulated through an explicit dependence of the vacuum energy density on the Hubble rate, $\rho_\Lambda = \rho_\Lambda(H)$, motivated by quantum field theory in curved space-time, the $\Lambda(t)$ CDM framework implements vacuum dynamics phenomenologically via a modified matter dilution law. At the background level and for small values of the model parameter α , the two models exhibit nearly equivalent expansion histories, leading to similar late-time cosmological signatures.

² For the original Chaplygin gas, $\alpha = 1$ and the EoS has the form $p = -A/\rho$.

parameter of the unified cosmic fluid, the effective DE EoS and deceleration parameters within the framework of the spatially flat $\Lambda(t)$ CDM model. We perform a detailed analysis of the dynamical behavior of the model by examining the expansion history of the universe, along with the temporal evolution of the total effective EoS parameter of the unified cosmic fluid, the effective DE EoS parameter, and the deceleration parameter.

Direct measurements of the Hubble expansion rate from cosmic chronometers provide a relatively model-independent probe of the late-time expansion history. When combined with baryon acoustic oscillation (BAO) measurements, these data enable a robust assessment of vacuum dynamics and spatial curvature, significantly reducing the parameter degeneracies present when $H(z)$ data are used alone. We apply Markov Chain Monte Carlo (MCMC) analysis to constrain the parameters of spatially flat and non-flat $\Lambda(t)$ CDM models and compare them with the standard spatially flat and non-flat Λ CDM scenarios, using $H(z)$ measurements [83–88] and combined $H(z)$ +BAO data from the Dark Energy Spectroscopic Instrument (DESI) Data Release 2 (DR2) [89]. To our knowledge, this represents the first observational analysis of the spatially flat and non-flat $\Lambda(t)$ CDM model using DESI DR2 BAO data. For model comparison, we employ several Bayesian statistical criteria and goodness-of-fit estimators, including $\Delta\chi_{\min}^2$, the Akaike Information Criterion (*AIC*), the corrected Akaike Information Criterion (*AICc*), the Bayesian Information Criterion (*BIC*) and the Akaike weights w_i .

Rather than claiming full resolution of the Hubble tension, our goal is to assess whether vacuum dynamics within the $\Lambda(t)$ CDM framework can alleviate the discrepancy between early and late-time determinations of H_0 .

This paper is organized as follows: Section II presents a description of the $\Lambda(t)$ CDM model; Section III discusses the derivation of the reconstructive formulas for the total effective EoS parameter of the unified cosmic fluid, the effective DE EoS parameter, and the deceleration parameter in the spatially flat $\Lambda(t)$ CDM model; Section IV considers the features of observational constraints on the parameters of the spatially flat and non-flat Λ CDM and $\Lambda(t)$ CDM models; Section V presents the results and analysis of the calculations; and Section VI summarizes the conclusions. We use the natural system of units here $c = k_B = 1$.

II. BACKGROUND DYNAMICS OF THE $\Lambda(t)$ CDM MODEL

We assumed that the flat, homogeneous and isotropic universe is described by the Friedmann–Lemaître–Robertson–Walker spacetime metric $ds^2 = dt^2 - a^2(t)d\mathbf{x}^2$, where t is a cosmic time; \mathbf{x} are the comoving coordinates; $a(t)$ is a scale factor, normalized to be unity at the present epoch $a_0 \equiv a(t_0) = 1$, so that $a = 1/(1+z)$, here z is the redshift.

Within the FLRW framework, which includes a component of pressureless matter with energy density ρ_m coupled to a dynamical vacuum-like energy density $\Lambda(t)$ depending on cosmic time, the first Friedmann equation (in units where $8\pi G/3 = 1$, with G being Newton’s gravitational constant) and the corresponding conservation equations read, respectively

$$3H^2 = \rho_m + \Lambda(t), \quad (1)$$

$$\dot{\rho}_m + 3H\rho_m = \Gamma\rho_m = -\dot{\Lambda}(t), \quad (2)$$

where the over-dot represents the derivative with respect to cosmic time, H is a Hubble parameter.

The dependence of the dynamical cosmological constant on the Hubble parameter is represented as [38, 39]

$$\Lambda(t) = \varrho H^{-2\alpha}, \quad \text{with } \varrho = 3(1 - \Omega_{m0})H_0^{2(1+\alpha)}, \quad (3)$$

here H_0 is a value of the Hubble parameter at the present epoch, $H_0 = 100h \text{ km s}^{-1}\text{Mpc}^{-1}$, h is the dimensionless Hubble parameter; Ω_{m0} is the matter density parameter at the present epoch. The constant α is the vacuum dynamics parameter (also acting as an interaction parameter), whose absolute value quantifies the strength of energy exchange between DE and matter over cosmic time. It parameterizes deviations from the Λ CDM model and characterizes the dynamical nature of the vacuum component. As mentioned above, this parameter is restricted to $\alpha > -1$.

The function Γ specifies the effective rate of matter creation for $\Gamma > 0$ and the annihilation rate for $\Gamma < 0$, and in this class of models takes the form of [38, 39]

$$\Gamma = -\alpha\varrho H^{-(2\alpha+1)}. \quad (4)$$

In the $\Lambda(t)$ CDM model, the general form of the normalized Hubble parameter, in which the DE and matter components are unified and parameterized by a power-law dependence on the vacuum dynamics parameter α , is given by [38, 39]

$$E(a) = \left[\left((1 - \Omega_{m0}) + \Omega_{m0}a^{-3(1+\alpha)} \right)^{\frac{1}{1+\alpha}} + \Omega_{r0}a^{-4} + \Omega_{k0}a^{-2} \right]^{1/2}, \quad (5)$$

where $E = H(a)/H_0$ is the normalized Hubble parameter; Ω_{r0} and Ω_{k0} denote the radiation and spatial curvature density parameters at the present epoch, respectively. In this paper, we consider the values $h = 0.6891$ and $\Omega_{m0} = 0.3038$ of [90].

Positive values of the vacuum dynamics parameter α , corresponding to a quintessence-like regime [2, 91], lead to a decreasing vacuum energy density that transfers energy to the matter sector, resulting in effective matter creation and cosmic expansion faster than in the standard Λ CDM model. In contrast, negative values of α ,

corresponding to a phantom-like regime [92, 93], produce an increasing vacuum energy density at the expense of matter, causing effective matter annihilation and slower cosmic expansion compared to the Λ CDM model. The limit $\alpha = 0$ recovers the standard Λ CDM scenario, in which the matter and vacuum components are conserved separately. By analyzing Eq. (5), it follows that in the early universe ($a \rightarrow 0$), the term proportional to $a^{-3(1+\alpha)}$ dominates the energy density, leading to $\rho(a) \propto a^{-3}$. In this regime, the unified matter–DE component behaves as pressureless matter, effectively mimicking cold DM and allowing for the formation of standard cosmic structures. At intermediate epochs, the expansion history encoded in $E(a)$ is governed by the competition between the matter-like term $\Omega_{m0}a^{-3(1+\alpha)}$, dominant at early times, and the constant contribution $(1 - \Omega_{m0}) \equiv \Omega_{DE0}$, which gradually becomes important and drives the departure from matter domination, signaling the onset of late-time accelerated expansion. In the asymptotic future ($a \gg 1$), the contribution of matter becomes negligible and Eq. (5) approaches a constant value, implying vacuum domination and an asymptotically de Sitter-like expansion.

A three-dimensional evolution of the Hubble parameter $H(a)$ in the spatially flat $\Lambda(t)$ CDM model, as a function of α and the scale factor a , is illustrated in Fig. 1, assuming $\Omega_{m0} = 0.3038$ and $H_0 = 68.91 \text{ km s}^{-1}\text{Mpc}^{-1}$ [90].

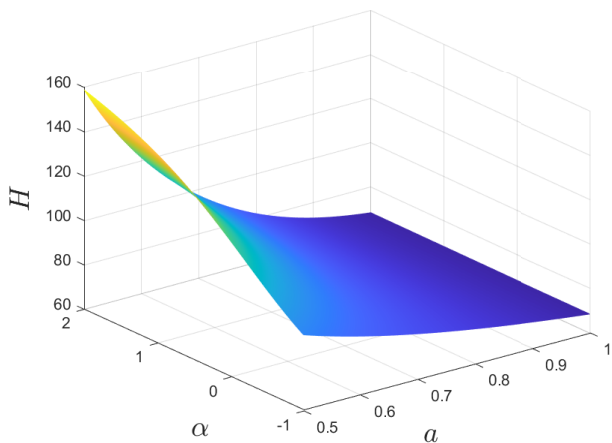


FIG. 1: Three-dimensional representation of the Hubble parameter $H(a)$ in the spatially flat $\Lambda(t)$ CDM model, shown in the $\alpha - a$ phase space, for $\Omega_{m0} = 0.3038$ and $H_0 = 68.91 \text{ km s}^{-1}\text{Mpc}^{-1}$ [90].

III. RECONSTRUCTION OF THE EFFECTIVE EOS PARAMETER OF THE UNIFIED COSMIC FLUID, THE DE EOS PARAMETER, AND THE DECELERATION PARAMETER

We derive the explicit form of the total effective EoS parameter of the unified cosmic fluid in the spatially flat

$\Lambda(t)$ CDM model, $w_{tot} = p_{tot}/\rho_{tot}$ (see Appendix A for details), which characterizes the combined behavior of matter and DE in the $\Lambda(t)$ CDM framework.

The total effective EoS parameter of the unified cosmic fluid is given by (see Eqs. (A9))

$$w_{tot}(a) = -1 + \frac{\Omega_{m0}a^{-3(1+\alpha)}}{1 - \Omega_{m0} + \Omega_{m0}a^{-3(1+\alpha)}}.$$

The asymptotic behavior of w_{tot} can be summarized as follows: in the early universe, $w_{tot}(a \rightarrow 0) \rightarrow 0$; at the present epoch, $w_{tot}(a = 1) = -(1 - \Omega_{m0}) = -\Omega_{DE0}$; and in the asymptotic future, $w_{tot}(a \gg 1) \rightarrow -1$. This sequence reflects the standard cosmological evolution from a matter dominated era ($w_{tot} \simeq 0$) to a vacuum dominated phase, ultimately approaching an asymptotic de Sitter state ($w_{tot} \rightarrow -1$). Consequently, despite the presence of vacuum dynamics, the $\Lambda(t)$ CDM model naturally reproduces the conventional dust \rightarrow vacuum domination \rightarrow de Sitter evolution, preserving the essential features of early time structure formation while slightly modifying the timing of late time cosmic acceleration.

We also derive the deceleration parameter and the effective DE EoS parameter, w_{DE} , treating DE as a distinct component in the spatially flat $\Lambda(t)$ CDM model (see Appendix B for details). This distinction is crucial, since w_{tot} and w_{DE} coincide only in the asymptotic future limit of complete DE domination, whereas at earlier times, including the present epoch, they generally differ due to the non-negligible contribution of matter.

In the spatially flat $\Lambda(t)$ CDM model, the deceleration parameter and the effective DE EoS parameter take, respectively, the following forms (see Eqs. (B4) and (B5))

$$q(a) = -1 + \frac{3}{2} \frac{\Omega_{m0}a^{-3(1+\alpha)}}{X},$$

$$w_{DE}(a) = -\frac{1 - \Omega_{m0}a^{-3(1+\alpha)}X^{-1}}{1 - \Omega_{m0}a^{-3}X^{-\frac{1}{1+\alpha}}}, \text{ with } \alpha \neq -1,$$

where $X = 1 - \Omega_{m0} + \Omega_{m0}a^{-3(1+\alpha)}$.

For $\alpha = 0$, the expression for the DE EoS parameter in Eq. (B5) reduces to that of the standard Λ CDM model, with $w_{DE}(a) = -1$. At the present epoch, *i.e.*, for $a = 1$, Eqs. (B4) and (B5) yield $q(a = 1) = \frac{3}{2}\Omega_{m0} - 1$ and $w_{DE}(a = 1) = -1$, respectively. By contrast, the effective EoS parameter of the unified cosmic fluid is today, according to Eq. (A9), $w_{tot}(a = 1) = -\Omega_{DE0}$ due to the residual matter contribution. Therefore, the $\Lambda(t)$ CDM model approaches the standard Λ CDM scenario only asymptotically in the future, rather than exactly at the present epoch.

IV. OBSERVATIONAL CONSTRAINTS OF THE $\Lambda(t)$ CDM AND Λ CDM MODELS

We perform observational constraints on the parameter sets $\mathbf{p} = \{H_0, \alpha, \Omega_{m0}\}$ and $\mathbf{p} = \{H_0, \alpha, \Omega_{m0}, \Omega_{k0}\}$ for the flat and non-flat $\Lambda(t)$ CDM models, respectively, and $\mathbf{p} = \{H_0, \Omega_{m0}\}$ and $\mathbf{p} = \{H_0, \Omega_{m0}, \Omega_{k0}\}$ for the flat and non-flat Λ CDM models, respectively. For this purpose, we applied 32 $H(z)$ measurements in the redshift range of $z \in [0.07, 1.965]$ [83–88], of which 15 measurements are correlated [94–96]. The covariance matrix for the correlated measurements we found at <https://gitlab.com/mmoresco/CCcovariance/>. In addition, we used 13 Baryon Acoustic Oscillation (BAO) measurements [89] from DESI DR2 in the redshift range $z \in [0.295, 2.330]$.

The priors for the parameters of the Λ CDM and $\Lambda(t)$ CDM models adopted in our analysis are presented in Table I.

TABLE I: Priors for the parameters.

Parameter	Priors
H_0	[None, None]
α	[-0.99, 1]
Ω_{m0}	[0.2, 0.6]
Ω_{k0}	[-0.6, 0.6]

We obtain the posterior distributions of the parameters of the Λ CDM and $\Lambda(t)$ CDM models using the MCMC method with the Cobaya software package [97]. To create plots and analyze the MCMC results, we applied the PYTHON GETDIST package [98].

For model selection based on the $H(z)$ data alone, we employ the corrected AICc, since the number of data points is relatively small compared to the number of free parameters. The AICc is defined as [99]

$$AICc = \chi_{\min}^2 + 2k + \frac{2k(k+1)}{n-k-1}, \quad (6)$$

where χ_{\min}^2 is the minimum chi-squared value, k denotes the number of free parameters, and n is the total number of data points. For the $H(z)$ data set ($n = 32$, corresponding to $n/k = 6.4-16 < 40$), the use of AICc is justified, as it corrects for the known tendency of the standard AIC to favor overly complex models in small-sample regimes [99].

For the combined $H(z)$ +BAO data set, the AIC is sufficient, as the correction becomes negligible. The AIC can be evaluated as [100]

$$AICc = \chi_{\min}^2 + 2k. \quad (7)$$

As an additional consistency check, we compute BIC, defined as [101]

$$BIC = \chi_{\min}^2 + k \ln n. \quad (8)$$

The comparison of the models is performed using the differences $\Delta AICc$ (or ΔAIC) and ΔBIC , defined relative to the model that minimizes the corresponding information criterion.

Furthermore, we evaluated the Akaike weights w_i [102]

$$w_i = \frac{\exp(-\Delta_i/2)}{\sum_{j=1}^R \exp(-\Delta_j/2)}, \quad (9)$$

where $\Delta_i = AICc_i - \min(AICc)$ (or $\Delta_i = AIC_i - \min(AIC)$), and R denotes the total number of models under consideration. These weights can be interpreted as the relative probability that a given model provides the best description of the data, in the sense of minimizing information loss, assuming that one of the candidate models is correct.

In addition, the quantities $\Delta\chi_{\min}^2 = \chi_{\min,i}^2 - \min(\chi_{\min}^2)$ and the reduced chi-squared, χ_{\min}^2/dof , are used to assess the goodness of fit of each model, where $\text{dof} = n - k$ is the number of degrees of freedom. All values of $\Delta\chi_{\min}^2$, $\Delta AICc$, ΔAIC , and ΔBIC are calculated with respect to the best-performing model within each data set separately, and Akaike weights are used to quantify the relative statistical support of competing models.

V. RESULTS AND DISCUSSIONS

A. Properties of the spatially flat $\Lambda(t)$ CDM model

1. Expansion of the universe

We numerically solve the first Friedmann equation Eq. (5), without the spatial curvature term, to study the expansion of the universe for the spatially flat $\Lambda(t)$ CDM model. The evolution of the normalized Hubble expansion rate as a function of the scale factor for different values of the vacuum dynamics parameter α is shown in Fig. 2. The normalized Hubble expansion rate decreases more rapidly for all values of the scale factor with an increase in the value of the vacuum dynamics parameter α . For $\alpha < 0$, the normalized Hubble expansion rate in the spatially flat $\Lambda(t)$ CDM model decreases more slowly than in the Λ CDM model. This evolution is similar to the evolution of the normalized Hubble expansion rate in phantom scalar field DE models. However, for $\alpha > 0$, the normalized Hubble expansion rate in the spatially flat $\Lambda(t)$ CDM model decreases faster than in the Λ CDM model, which corresponds to the behavior of the normalized Hubble expansion rate in quintessence scalar field DE models.

2. Analysis of the reconstructed effective and DE EoS parameters and the deceleration parameter

The numerical solution of Eq. (B5) for the effective reconstructed DE EoS parameter in the spatially flat

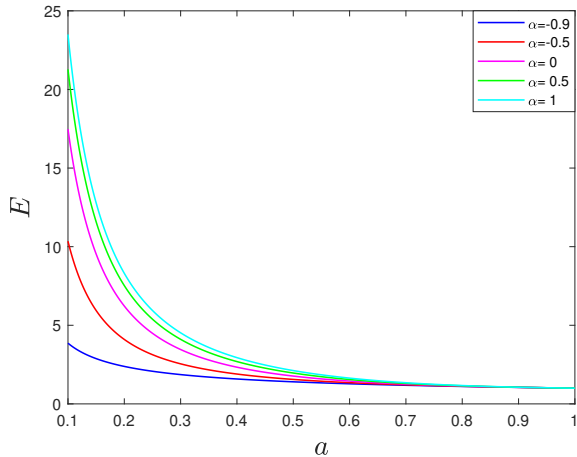


FIG. 2: Normalized Hubble expansion rate in the spatially flat $\Lambda(t)$ CDM model as a function of the scale factor for different values of the vacuum dynamics parameter α .

$\Lambda(t)$ CDM model for the positive values of the vacuum dynamics parameter α , which corresponds to quintessence-like DE, in the scale factor range $a \in [0.1, 1]$ is presented in Fig. 3. The evolution of the DE EoS parameter $w_{DE}(a)$ shows that, at early times ($a \ll 1$), the unified dark component behaves as pressureless matter, with $w(a) \simeq 0$, independently of the value of α . As the universe expands, $w_{DE}(a)$ evolves toward negative values and enters the quintessence regime $-1 < w_{DE}(a) < -1/3$. We find that increasing positive values of α delay the transition from the matter dominated epoch to the DE dominated epoch. In particular, for larger values of α , the deviation of $w_{DE}(a)$ from its matter-like value $w_{DE} \simeq 0$ and its subsequent transition to negative values occur at later cosmic times. All evolutionary trajectories converge to $w = -1$ at the present epoch, *i.e.*, the $\Lambda(t)$ CDM model effectively reduces to the standard Λ CDM scenario at late times. Although the $\Lambda(t)$ CDM model does not correspond to canonical scalar-field quintessence³, its effective evolution of the

³ While the present analysis is restricted to the quintessence regime ($\alpha > 0$), the same theoretical framework can be naturally extended to the phantom DE case ($\alpha < 0$). In this regime, the cosmological evolution exhibits qualitatively different behavior. In particular, the transition between the matter-dominated and DE-dominated stages occurs at earlier cosmic times as α decreases. The interaction between the vacuum component and matter can lead to effective matter creation, resulting in a slower dilution of the matter energy density compared to the standard scaling, $\rho_m \propto a^{-3}$. Consequently, dark energy may become dynamically relevant at earlier epochs due to the reduced effective matter content at late times. For sufficiently negative values of α , the accelerated expansion can become increasingly pronounced, potentially giving rise to future cosmological scenarios characterized by very rapid expansion, such as Big Rip-like behavior.

DE EoS parameter for $\alpha > 0$ resembles that of freezing quintessence models, with $w(a)$ gradually approaching -1 at late times.

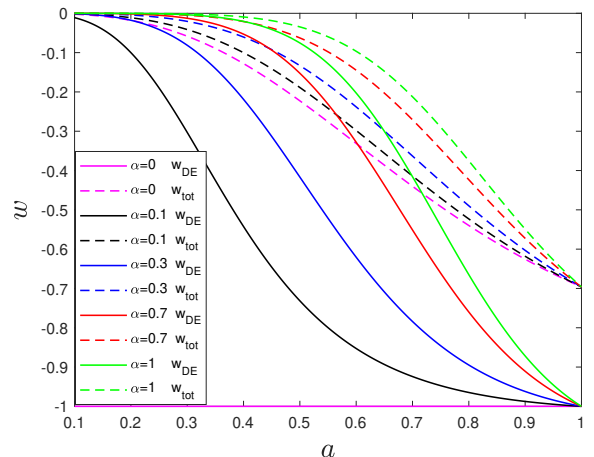


FIG. 3: Total effective EoS parameter of the unified cosmic fluid (solid lines) and the effective DE EoS parameter (dashed lines) as functions of the scale factor for different values of the vacuum dynamics parameter α in the spatially flat $\Lambda(t)$ CDM model.

The numerical solution of Eq. (A9) for the total effective EoS parameter of the unified cosmic fluid in the spatially flat $\Lambda(t)$ CDM model, for positive values of the vacuum dynamics parameter α , is shown in Fig. 3. By comparing the evolution of w_{tot} with that of the effective DE EoS parameter w_{DE} , we find that, similarly to w_{DE} , increasing positive values of α shift the transition from the matter-dominated epoch to the DE dominated epoch to later times. However, in contrast to w_{DE} , the transition in the evolution of w_{tot} from matter domination to DE domination occurs later than that of w_{DE} for the same fixed value of α . For $\alpha = 0$, the total effective EoS parameter evolves as

$$w_{tot}(a) = -1 + \frac{\Omega_{m0}a^{-3}}{1 - \Omega_{m0} + \Omega_{m0}a^{-3}}.$$

All w_{tot} trajectories, independently of the value of α , converge at the present epoch to $w_{tot}(a = 1) = \Omega_{m0} - 1$. In our analysis, assuming $\Omega_{m0} = 0.3038$ [90], this yields $w_{tot}(a = 1) = -0.6962$.

The numerical solution of Eq. (B4) for the reconstructed deceleration parameter $q(a)$ in the spatially flat $\Lambda(t)$ CDM model, assuming positive values of the vacuum dynamics parameter α , over the scale factor range $a \in [0.1, 1]$ is presented in Fig. 4. At early times,

A detailed investigation of such late-time singularities, however, lies beyond the scope of the present work.

$q(a) > 0$, indicating a decelerated expansion dominated by matter. As the vacuum component becomes dynamically significant, $q(a)$ decreases and eventually crosses zero, marking the transition from decelerated to accelerated expansion of the universe. Our results indicate that increasing $\alpha > 0$ shifts this transition to later epochs, implying that a stronger vacuum–matter interaction delays the onset of cosmic acceleration. Despite these differences in evolutionary trajectories, all solutions converge to the same current value of the deceleration parameter, $q_0 = -0.5443$, corresponding to $\Omega_{m0} = 0.3038$ [90].

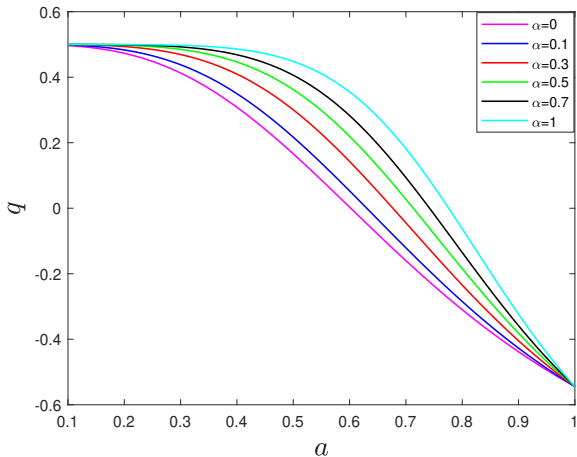


FIG. 4: Evolution of the deceleration parameter as a function of the scale factor for different values of the vacuum dynamics parameter α in the spatially flat $\Lambda(t)$ CDM model.

B. Observational constraints of the $\Lambda(t)$ CDM and Λ CDM models

Based on the MCMC analysis, we obtain the one-dimensional likelihood distributions and the 1σ , 2σ , and 3σ confidence contours for the model parameters using 32 $H(z)$ measurements for the spatially flat $\Lambda(t)$ CDM model (left panel of Fig. 5) and the non-flat $\Lambda(t)$ CDM model (right panel of Fig. 5). Using the combined dataset of 32 $H(z)$ and 13 BAO measurements, we further derive the joint 1σ , 2σ , and 3σ confidence contours for the spatially flat and non-flat $\Lambda(t)$ CDM models (Fig. 6), as well as for the standard flat Λ CDM model and its non-flat extension (Fig. 7).

The one-dimensional posterior median values and their 1σ uncertainties for the flat and non-flat Λ CDM and $\Lambda(t)$ CDM models, obtained from various combinations of $H(z)$ and $H(z)$ +BAO data, are summarized in Table II. Using $H(z)$ data alone leads to relatively large uncertainties in all models, particularly for the spatially non-flat $\Lambda(t)$ CDM scenario. For this model, we find $H_0 = 61.08^{+9.60}_{-6.38}$ km s⁻¹Mpc⁻¹, $\Omega_{m0} = 0.214^{+0.237}_{-0.173}$,

$\Omega_{k0} = 0.236^{+0.253}_{-0.274}$, and $\alpha = 0.475^{+1.633}_{-0.835}$, indicating weak constraints and strong parameter degeneracies. In contrast, the flat $\Lambda(t)$ CDM model and both flat and non-flat Λ CDM models provide $H_0 \sim 67$ – 68 km s⁻¹Mpc⁻¹ with broader uncertainties compared to the combined datasets, while the parameter α remains statistically consistent with zero in the spatially flat and non-flat $\Lambda(t)$ CDM models. The inclusion of BAO data significantly tightens the parameter constraints for all models (see Table II). For the non-flat $\Lambda(t)$ CDM model, we find $H_0 = 67.76 \pm 1.66$ km s⁻¹Mpc⁻¹, $\Omega_{m0} = 0.328^{+0.049}_{-0.045}$, $\Omega_{k0} = 0.009^{+0.050}_{-0.044}$, and $\alpha = -0.081 \pm 0.133$, favoring a spatially flat universe and a matter density parameter Ω_{m0} compatible with that of the standard Λ CDM model. Similarly, the flat $\Lambda(t)$ CDM model results in $H_0 = 67.87 \pm 0.91$ km s⁻¹Mpc⁻¹, $\Omega_{m0} = 0.344^{+0.040}_{-0.035}$, and $\alpha = -0.127 \pm 0.097$, with the inclusion of BAO data substantially reducing uncertainties in α while maintaining consistency with zero. In both spatially flat and non-flat Λ CDM models, BAO data reduce the uncertainties in the H_0 and Ω_{m0} parameters by a factor of 3–6 and constrain the Ω_{k0} parameter close to zero; in the spatially non-flat Λ CDM scenario, $\Omega_{k0} = 0.024^{+0.043}_{-0.038}$, again favoring a nearly flat geometry. Consequently, the inclusion of BAO data reduces the Hubble tension with the Planck CMB result⁴ to less than 1σ for all models, and reduce the tension with SH0ES to ~ 2.6 – 3.2σ . Thus, the inclusion of BAO data substantially reduces parameter degeneracies and leads to mutually consistent cosmological parameter estimates across all considered models, while the vacuum dynamics parameter α remains statistically consistent with zero in spatially flat and non-flat Λ CDM models.

We evaluated the performance of the flat and non-flat $\Lambda(t)$ CDM and Λ CDM models using goodness-of-fit statistics and information criteria based on the $H(z)$ and combined $H(z)$ +BAO data sets (see Tables III–IV). All models provide an excellent fit to the $H(z)$ data, with $\chi^2_{\min}/\text{dof} \simeq 0.5$ (see Table III). When using $H(z)$ data alone, both flat and non-flat $\Lambda(t)$ CDM models suffer from large uncertainties in their cosmological parameters, with the non-flat scenario exhibiting weak constraints on H_0 , Ω_{m0} , Ω_{k0} , and α parameters, reflecting strong parameter degeneracies (see Table II). The flat $\Lambda(t)$ CDM model provides comparatively tighter constraints; however, the vacuum dynamics parameter α remains consistent with zero within the 1σ , indicating that there are no statistically significant deviations from the standard Λ CDM

⁴ We emphasize that the quoted Planck CMB constraint on H_0 is obtained under the assumption of the standard Λ CDM cosmological model. A dedicated CMB analysis within the $\Lambda(t)$ CDM framework would, in general, yield different parameter estimates and could alter the level of statistical agreement with the Planck CMB result. Such an analysis is beyond the scope of the present work, and the Planck CMB constraint is therefore used here solely as a reference benchmark.

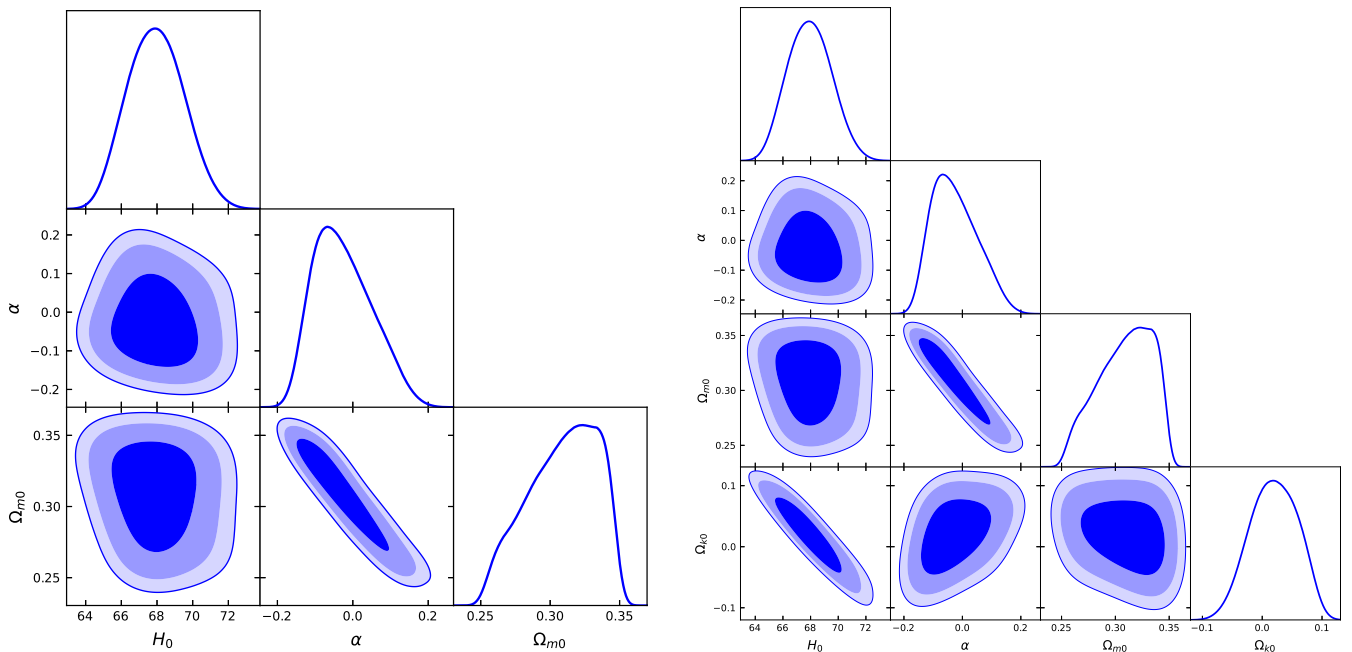


FIG. 5: One-dimensional likelihoods and 1σ , 2σ and 3σ confidence levels contours constraints on the parameters of the $\Lambda(t)$ CDM model from $H(z)$ measurements: for the flat space (left panel) and the non-flat space (right panel).

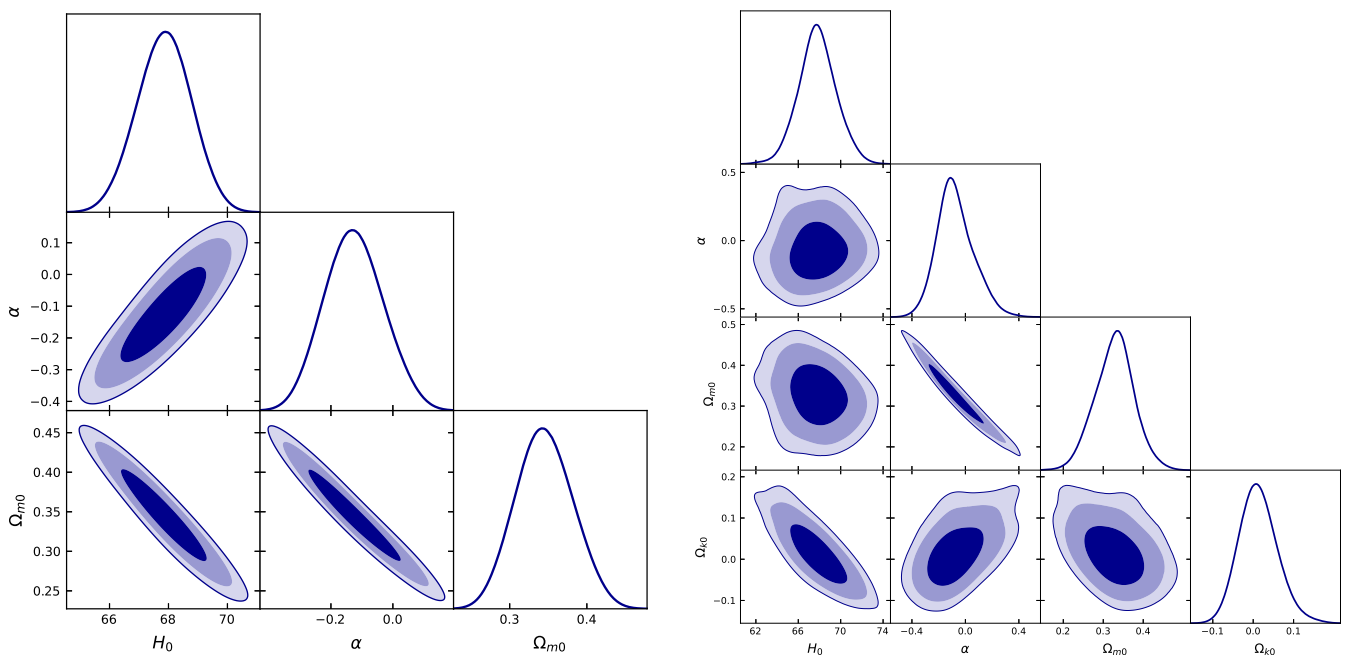


FIG. 6: One-dimensional likelihoods and 1σ , 2σ and 3σ confidence levels contours constraints on the parameters of the $\Lambda(t)$ CDM model from the combination of $H(z)$ + BAO measurements: for the flat space (left panel) and the non-flat space (right panel).

model.

A comparison based on information criteria (AIC_c and BIC) reveals a clear preference for the flat Λ CDM model. Although the non-flat $\Lambda(t)$ CDM model achieves the lowest χ^2_{\min} value when using $H(z)$ data alone, this improvement is insufficient to compensate for the penalty associ-

ated with the additional parameter α . When BAO data are included, the discriminating power of the information criteria increases significantly, with all models continuing to provide comparably good fits ($\chi^2_{\min}/\text{dof} \simeq 0.6$). Nevertheless, both AIC and BIC strongly favor the flat Λ CDM model. Although the flat $\Lambda(t)$ CDM model attains

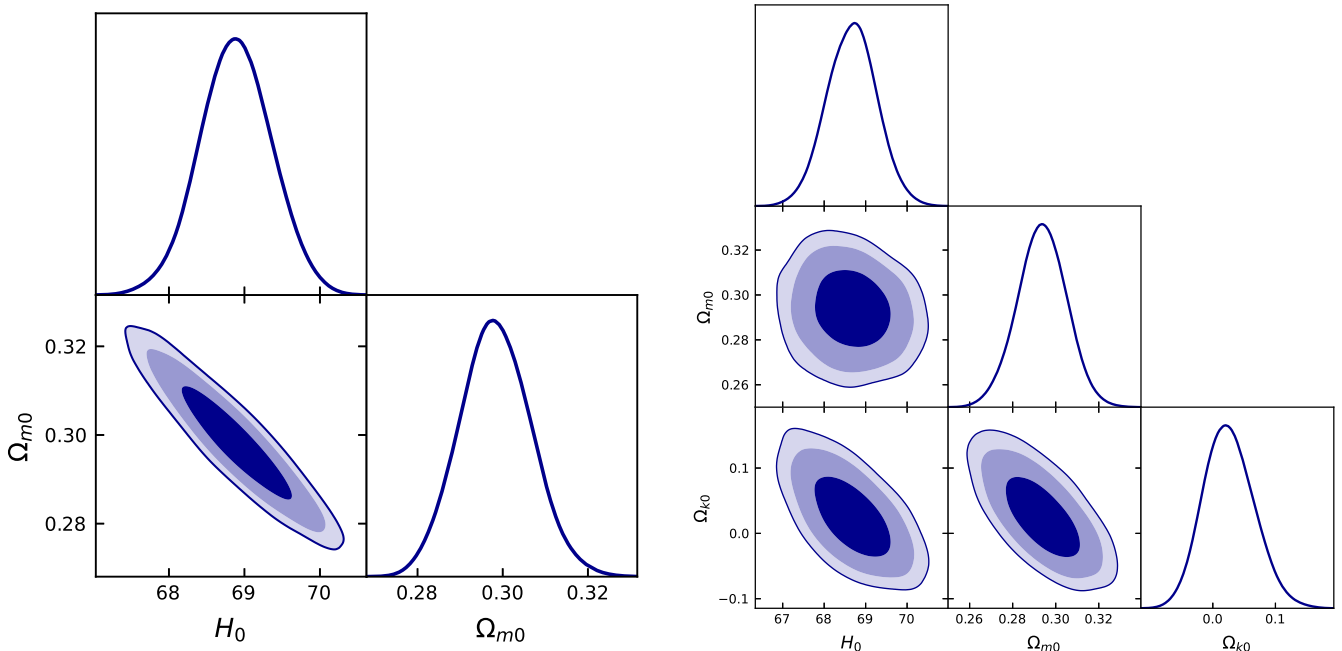


FIG. 7: One-dimensional likelihoods and 1σ , 2σ and 3σ confidence levels contours constraints on the parameters of the Λ CDM model from the combination of $H(z)$ + BAO measurements: for the flat space (left panel) and the non-flat space (right panel).

the minimum χ^2_{\min} value in this case, the additional parameter α is penalized by the information criteria, leading to a clear preference for the simpler Λ CDM scenario. The Akaike weights indicate that the flat Λ CDM model carries approximately 44–58% of the total statistical support, while extended models with vacuum dynamics or spatial curvature receive substantially less weight. As a result, the inclusion of BAO data significantly reduces parameter degeneracies and reinforces the preference for standard flat Λ CDM cosmology.

VI. CONCLUSIONS

We analyze the dynamical behavior of the spatially flat $\Lambda(t)$ CDM model by studying the expansion history of the universe through the normalized Hubble rate $E(a)$, including the effective EoS parameter of the unified cosmic fluid $w_{tot}(a)$, the effective DE EoS parameter $w_{DE}(a)$, and the deceleration parameter $q(a)$. In the spatially flat $\Lambda(t)$ CDM framework, the vacuum dynamics parameter α plays a key role in shaping cosmic expansion. For $\alpha < 0$, the expansion rate $E(a)$ decreases more slowly than in the standard Λ CDM model, resembling a phantom-like DE behavior, while for $\alpha > 0$, $E(a)$ decreases faster, similar to quintessence-like DE models (see Fig. 2).

The explicit expressions for $w_{tot}(a)$, $w_{DE}(a)$ (Eqs. A9 and B5, respectively), and $q(a)$ (Eq. B4) show that positive values of α , corresponding to a freezing quintessence-like vacuum, systematically delay the onset of cosmic acceleration. This behavior is consistently reflected in

the evolution of $w_{tot}(a)$ and $w_{DE}(a)$, which remain close to zero for a longer period before entering the negative-pressure regime (Fig. 3), as well as in the evolution of $q(a)$, for which the transition from deceleration to acceleration occurs at later epochs (Fig. 4). In contrast to $w_{DE}(a)$, the transition in the evolution of $w_{tot}(a)$ from matter domination to DE domination occurs later for the same fixed value of α , reflecting the contribution of residual matter to the total cosmic fluid.

The contribution of residual matter to $w_{tot}(a)$ is evident both in the limit $\alpha = 0$, where the spatially flat $\Lambda(t)$ CDM model reduces to the standard Λ CDM scenario with $w_{DE}(a) = -1$, while $w_{tot}(a) = -1 + \frac{\Omega_{m0}a^{-3}}{(1-\Omega_{m0}+\Omega_{m0}a^{-3})}$, and at the present epoch, where all trajectories of $w_{DE}(a)$ converge to $w_{DE}(a=1) = -1$, while $w_{tot}(a=1) = -1 + \Omega_{m0} = -\Omega_{DE0}$. Consequently, the $\Lambda(t)$ CDM model approaches the standard Λ CDM scenario only asymptotically in the future, rather than reproducing it exactly at the present epoch.

Despite these late-time modifications, the $\Lambda(t)$ CDM model preserves standard matter-like behavior at early times, ensuring consistency with large-scale structure formation. Overall, the $\Lambda(t)$ CDM model represents a physically viable extension of the standard Λ CDM framework, in which vacuum dynamics shifts the epoch of cosmic acceleration without altering the early evolution of the universe.

Based on MCMC analysis, we constrain the parameters of both spatially flat and non-flat $\Lambda(t)$ CDM models using 32 $H(z)$ measurements from cosmic chronometers ($z \in [0.07, 1.965]$) and 13 BAO measurements from DESI

TABLE II: One-dimensional posterior median values of the model parameters with their 1σ uncertainties for the flat and non-flat $\Lambda(t)$ CDM and Λ CDM models from the $H(z)$ and $H(z)$ +BAO datasets.

Model	Data	H_0^a	Ω_{m0}	Ω_{k0}	α
Flat $\Lambda(t)$ CDM	$H(z)$	67.91 ± 1.62	$0.312^{+0.024}_{-0.031}$	–	$-0.035^{+0.093}_{-0.071}$
	$H(z)$ +BAO	67.87 ± 0.91	$0.344^{+0.040}_{-0.035}$	–	-0.127 ± 0.097
Non-flat $\Lambda(t)$ CDM	$H(z)$	$61.08^{+9.60}_{-6.38}$	$0.214^{+0.237}_{-0.173}$	$0.236^{+0.253}_{-0.274}$	$0.475^{+1.633}_{-0.835}$
	$H(z)$ +BAO	67.76 ± 1.66	$0.328^{+0.049}_{-0.045}$	$0.009^{+0.050}_{-0.044}$	-0.081 ± 0.133
Flat Λ CDM	$H(z)$	67.66 ± 3.05	$0.326^{+0.067}_{-0.054}$	–	–
	$H(z)$ +BAO	68.90 ± 0.49	0.298 ± 0.009	–	–
Non-flat Λ CDM	$H(z)$	67.99 ± 3.83	$0.350^{+0.124}_{-0.133}$	$-0.062^{+0.404}_{-0.354}$	–
	$H(z)$ +BAO	68.68 ± 0.60	0.294 ± 0.011	$0.024^{+0.043}_{-0.038}$	–

^a km s⁻¹Mpc⁻¹

TABLE III: Goodness-of-fit and model comparison criteria for the flat and non-flat $\Lambda(t)$ CDM and Λ CDM models, based on the $H(z)$ data.

Model	χ^2_{\min}	$\Delta\chi^2_{\min}$	dof	χ^2_{\min}/dof	AICc	BIC	ΔAICc	ΔBIC	w_i
Flat $\Lambda(t)$ CDM	14.68	0.57	29	0.506	21.54	25.08	2.39	3.42	0.177
Non-flat $\Lambda(t)$ CDM	14.11	0.00	28	0.504	23.59	27.97	4.45	6.31	0.063
Flat Λ CDM	14.73	0.62	30	0.491	19.14	21.66	0.00	0.00	0.584
Non-flat Λ CDM	14.69	0.58	29	0.507	21.55	25.09	2.40	3.43	0.176

TABLE IV: Goodness-of-fit and model comparison criteria for the flat and non-flat $\Lambda(t)$ CDM and Λ CDM models, based on the $H(z)$ + BAO data.

Model	χ^2_{\min}	$\Delta\chi^2_{\min}$	dof	χ^2_{\min}/dof	AIC	BIC	ΔAIC	ΔBIC	w_i
Flat $\Lambda(t)$ CDM	24.44	0.00	42	0.582	30.44	35.86	0.99	2.80	0.269
Non-flat $\Lambda(t)$ CDM	24.47	0.03	41	0.597	32.47	39.70	3.02	6.63	0.097
Flat Λ CDM	25.45	1.01	43	0.592	29.45	33.06	0.00	0.00	0.441
Non-flat Λ CDM	25.10	0.66	42	0.598	31.10	36.52	1.65	3.46	0.193

DR2 ($z \in [0.295, 2.330]$). The one-dimensional likelihoods and 1σ , 2σ , and 3σ confidence contours from $H(z)$ alone and in combination $H(z)$ +BAO data are shown in Figs. 5–7. Using $H(z)$ data alone leads to large uncertainties, particularly in the non-flat $\Lambda(t)$ CDM model, where strong parameter degeneracies are present. The vacuum dynamics parameter α remains statistically consistent with zero in all $\Lambda(t)$ CDM scenarios.

The inclusion of BAO data substantially tightens parameter constraints for all models. For the non-flat $\Lambda(t)$ CDM model, we find $H_0 = 67.76 \pm 1.66$ km s⁻¹Mpc⁻¹, $\Omega_{m0} = 0.328^{+0.049}_{-0.045}$, $\Omega_{k0} = 0.009^{+0.050}_{-0.044}$, and $\alpha = -0.081 \pm 0.133$, favoring a nearly flat universe with matter density parameter Ω_{m0} compatible with the standard Λ CDM model. The flat $\Lambda(t)$ CDM model yields similar values with slightly tighter constraints. In both flat and non-flat Λ CDM models, the BAO data reduce the uncertainties in the H_0 and Ω_{m0} parameters by a factor of 3–6 and constrain the curvature density parameter Ω_{k0} close to zero. Consequently, the Hubble tension with Planck CMB measurements is reduced to below 1σ , and the tension with SH0ES decreases to ~ 2.6 – 3.2σ .

The fit and information criteria (*AICc* and *BIC*) in-

dicating a clear preference for the flat Λ CDM model. Although the $\Lambda(t)$ CDM models, particularly the non-flat case, can achieve slightly lower χ^2_{\min} values, the additional parameter α is penalized, resulting in less statistical support. The Akaike weights show that the flat Λ CDM model accounts for 44 – 58% of the total support, with extended models receiving substantially less. As a result, the inclusion of BAO data reduces parameter degeneracies and drives all models toward a spatially flat universe with parameters consistent with the standard Λ CDM model.

Appendix A: Derivation of the total effective EoS parameter of the unified cosmic fluid in the spatially flat $\Lambda(t)$ CDM model

For the unified cosmic fluid, the effective EoS parameter is defined as

$$w_{tot}(a) = -1 - \frac{1}{3} \frac{d \ln \rho_{tot}}{d \ln a}. \quad (\text{A1})$$

Since the total energy density scales as $\rho_{tot} \propto E^2(a)$, where the dimensionless Hubble parameter $E(a)$ is de-

defined in Eq. (5) under the assumptions $\Omega_{r0} = 0$ and $\Omega_{k0} = 0$, this expression can be rewritten as

$$w_{tot}(a) = -1 - \frac{1}{3} \frac{d \ln E^2}{d \ln a}. \quad (\text{A2})$$

Using

$$\ln E^2 = \frac{1}{1+\alpha} \ln X, \quad (\text{A3})$$

one finds

$$\frac{d \ln E^2}{d \ln a} = \frac{1}{1+\alpha} \frac{1}{X} \frac{dX}{d \ln a}, \quad (\text{A4})$$

where

$$X = (1 - \Omega_{m0}) + \Omega_{m0} a^{-3(1+\alpha)}. \quad (\text{A5})$$

The derivative of X with respect to $\ln a$ is given by

$$\frac{dX}{d \ln a} = -3(1+\alpha) \Omega_{m0} a^{-3(1+\alpha)}. \quad (\text{A6})$$

Substituting this result into Eq. (A4), we obtain

$$\frac{d \ln E^2}{d \ln a} = -\frac{3\Omega_{m0} a^{-3(1+\alpha)}}{X}, \quad (\text{A7})$$

which, when inserted into Eq. (A2), yields the expression for the unified total EoS parameter

$$w_{tot}(a) = -1 + \frac{\Omega_{m0} a^{-3(1+\alpha)}}{X}. \quad (\text{A8})$$

Equivalently, Eq. (A8) can be written as

$$w_{tot}(a) = -1 + \frac{\Omega_{m0} a^{-3(1+\alpha)}}{1 - \Omega_{m0} + \Omega_{m0} a^{-3(1+\alpha)}}. \quad (\text{A9})$$

Appendix B: Derivation of the effective DE EoS and deceleration parameters in the spatially flat $\Lambda(t)$ CDM model

In a spatially flat, radiation-free universe ($\Omega_{k0} = \Omega_{r0} = 0$), the effective dark DE EoS parameter can be recon-

structed from the deceleration parameter $q(a)$ as [103]

$$w_{DE}(a) = \frac{2q(a) - 1}{3(1 - \Omega_m(a))}, \quad \text{with} \quad \Omega_m(a) = \frac{\Omega_{m0} a^{-3}}{E^2(a)}. \quad (\text{B1})$$

The deceleration parameter is defined as

$$q(a) = -1 - a \frac{d \ln H}{da}. \quad (\text{B2})$$

Using Eq. (5) and Eq. (A5), the derivative with respect to the scale factor is determined as

$$\begin{aligned} \frac{d \ln H}{da} &= \frac{1}{E} \frac{dE}{da} = \frac{1}{2(1+\alpha)} X^{-1} \frac{dX}{da} = \\ &= \frac{1}{2(1+\alpha)} X^{-1} \left[-3(1+\alpha) \Omega_{m0} a^{-3(1+\alpha)-1} \right] = \\ &= -\frac{3}{2} \frac{\Omega_{m0} a^{-3(1+\alpha)-1}}{X}. \end{aligned} \quad (\text{B3})$$

This gives the deceleration parameter

$$q(a) = -1 - a \frac{d \ln H}{da} = -1 + \frac{3}{2} \frac{\Omega_{m0} a^{-3(1+\alpha)}}{X}. \quad (\text{B4})$$

Substituting Eq. (B4) into Eq. (B1), we obtain the explicit form of the DE EoS parameter in the $\Lambda(t)$ CDM model

$$w_{DE}(a) = -\frac{1 - \Omega_{m0} a^{-3(1+\alpha)} X^{-1}}{1 - \Omega_{m0} a^{-3} X^{-\frac{1}{1+\alpha}}}, \quad \text{with} \quad \alpha \neq -1. \quad (\text{B5})$$

This expression naturally reduces to the standard Λ CDM limit $w_{DE} = -1$ when $\alpha = 0$.

[1] P. J. E. Peebles, *Astrophys. J.* **284**, 439 (1984).
[2] P. J. E. Peebles and B. Ratra, *Rev. Mod. Phys.* **75**, 559 (2003).
[3] M. Lopez-Corredoira, arXiv:2307.10606 (2023).
[4] N. Aghanim et al. (Planck), *Astron. Astrophys.* **641**, A1 (2020).
[5] N. Aghanim et al. (Planck), *Astron. Astrophys.* **641**, A6 (2020).
[6] S. Aiola et al. (ACT), *JCAP* **12**, 047 (2020).
[7] S. Alam et al. (eBOSS), *Phys. Rev. D* **103**, 083533

(2021).
[8] L. Perivolaropoulos and F. Skara, *New Astron. Rev.* **95**, 101659 (2022).
[9] E. Di Valentino, *Universe* **8**, 399 (2022).
[10] E. Abdalla et al., *JHEAp* **34**, 49 (2022).
[11] P. J. E. Peebles, *Annals Phys.* **447**, 169159 (2022).
[12] S. Vagnozzi, *Universe* **9**, 393 (2023).
[13] A. G. Riess et al., *Astrophys. J. Lett.* **934**, L7 (2022).
[14] P. J. Steinhardt, L.-M. Wang, and I. Zlatev, *Phys. Rev. D* **59**, 123504 (1999).

- [15] J. Garriga and A. Vilenkin, *Phys. Rev. D* **64**, 023517 (2001).
- [16] N. Dalal, K. Abazajian, E. Jenkins, and A. V. Manohar, *Phys. Rev. Lett.* **87**, 141302 (2001).
- [17] M. Ishak, *Foundations of Physics* **37**, 1470 (2007).
- [18] G. D. Starkman and R. Trotta, *Phys. Rev. Lett.* **97**, 201301 (2006).
- [19] I. Maor, L. Krauss, and G. Starkman, *Phys. Rev. Lett.* **100**, 041301 (2008).
- [20] J. Martin, *Comptes Rendus Physique* **13**, 566 (2012).
- [21] J. Zheng, Y. Chen, T. Xu, and Z.-H. Zhu, arXiv:2107.08916 (2021).
- [22] C. Wetterich, *Astron. Astrophys.* **301**, 321 (1995).
- [23] L. Amendola, *Mon. Not. Roy. Astron. Soc.* **312**, 521 (2000).
- [24] L. Amendola, *Phys. Rev.* **D62**, 043511 (2000).
- [25] W. Zimdahl and D. Pavon, *Phys. Lett.* **B521**, 133 (2001).
- [26] X. Liu, S. Tsujikawa, and K. Ichiki, *Phys. Rev. D* **109**, 043533 (2024).
- [27] W. Yang, S. Pan, E. Di Valentino, R. C. Nunes, S. Vagnozzi, and D. F. Mota, *JCAP* **09**, 019 (2018).
- [28] E. Di Valentino, A. Melchiorri, O. Mena, and S. Vagnozzi, *Phys. Dark Univ.* **30**, 100666 (2020).
- [29] E. Di Valentino, A. Melchiorri, O. Mena, and S. Vagnozzi, *Phys. Rev. D* **101**, 063502 (2020).
- [30] R. C. Nunes and E. Di Valentino, *Phys. Rev. D* **104**, 063529 (2021).
- [31] E. Di Valentino, O. Mena, S. Pan, L. Visinelli, W. Yang, A. Melchiorri, D. F. Mota, A. G. Riess, and J. Silk, *Class. Quant. Grav.* **38**, 153001 (2021).
- [32] A. Bernui, E. Di Valentino, W. Giarè, S. Kumar, and R. C. Nunes, *Phys. Rev. D* **107**, 103531 (2023).
- [33] G. A. Hoerning, R. G. Landim, L. O. Ponte, R. P. Rolim, F. B. Abdalla, and E. Abdalla, *Phys. Rev. D* **112**, 023523 (2025).
- [34] E. M. Teixeira, R. Daniel, N. Frusciante, and C. van de Bruck, *Phys. Rev. D* **108**, 084070 (2023).
- [35] Y. Zhai, W. Giarè, C. van de Bruck, E. Di Valentino, O. Mena, and R. C. Nunes, *JCAP* **07**, 032 (2023).
- [36] S. Pan and W. Yang, arXiv:2310.07260 (2023).
- [37] A. Blanchard, arXiv:2505.06244 (2025).
- [38] M. Benetti, W. Miranda, H. A. Borges, C. Pigozzo, S. Carneiro, and J. S. Alcaniz, *JCAP* **12**, 023 (2019).
- [39] M. Benetti, H. Borges, C. Pigozzo, S. Carneiro, and J. Alcaniz, *JCAP* **08**, 014 (2021).
- [40] H. A. Borges, C. Pigozzo, P. Hepp, L. O. Baraúna, and M. Benetti, *JCAP* **06**, 009 (2023).
- [41] M. Koussour, N. Myrzakulov, and J. Rayimbaev, *Adv. Space Res.* **74**, 1343 (2024).
- [42] M. Benetti, P. T. Z. Seidel, C. Pigozzo, I. P. R. Baranov, S. Carneiro, and J. C. Fabris, *JCAP* **06**, 046 (2025).
- [43] Y. Yang, Y. Wang, and X. Dai, *Eur. Phys. J. C* **85**, 224 (2025).
- [44] G. di Donato and L. Pilo, *Phys. Rev. D* **111**, 064081 (2025).
- [45] P. A. S. Guillen, J. F. de Jesus, and R. V. d. C. Lima, arXiv:2512.14578 (2025).
- [46] I. L. Shapiro, J. Sola, C. Espana-Bonet, and P. Ruiz-Lapuente, *Physics Letters B* **574**, 149 (2003).
- [47] J. Sola, A. Gomez-Valent, and J. de Cruz Pérez, *Mod. Phys. Lett. A* **32**, 1750054 (2017).
- [48] J. Sola Peracaula, A. Gomez-Valent, and J. de Cruz Pérez, *Phys. Dark Univ.* **25**, 100311 (2019).
- [49] J. Sola Peracaula, *Phil. Trans. Roy. Soc. Lond. A* **380**, 20210182 (2022).
- [50] C. Moreno-Pulido and J. Sola Peracaula, *The European Physical Journal C* **82**, 551 (2022).
- [51] C. Moreno-Pulido and J. S. Peracaula, *The European Physical Journal C* **82**, 1137 (2022).
- [52] J. Sola Peracaula, A. Gomez-Valent, J. de Cruz Pérez, and C. Moreno-Pulido, *Universe* **9**, 262 (2023).
- [53] C. Moreno-Pulido, J. Sola Peracaula, and S. Cheraghchi, *Eur. Phys. J. C* **83**, 637 (2023).
- [54] J. Solà Peracaula, À. González-Fuentes, and C. Moreno-Pulido, arXiv:2601.05218 (2026).
- [55] S. Chaplygin, *Sci. Mem. Moscow Univ. Math. Phys.* **21**, 1 (1904).
- [56] N. Bilic, G. B. Tupper, and R. D. Viollier, *Phys. Lett. B* **535**, 17 (2002).
- [57] R. R. Caldwell, W. Komp, L. Parker, and D. A. T. Vanzella, *Phys. Rev. D* **73**, 023513 (2006).
- [58] H. Benaoum, *Universe* **8**, 340 (2022).
- [59] P. P. Avelino, L. M. G. Beca, J. P. M. de Carvalho, and C. J. A. P. Martins, *JCAP* **09**, 002 (2003).
- [60] U. Debnath, A. Banerjee, and S. Chakraborty, *Class. Quant. Grav.* **21**, 5609 (2004).
- [61] Z.-K. Guo and Y.-Z. Zhang, *Phys. Lett. B* **645**, 326 (2007).
- [62] R. Banerjee and S. Ghosh, *Mod. Phys. Lett. A* **21**, 1511 (2006).
- [63] S. del Campo and R. Herrera, *Phys. Lett. B* **665**, 100 (2008).
- [64] J. Lu, L. Xu, B. Chang, and Y. Gui, *Int. J. Mod. Phys. D* **18**, 1741 (2009).
- [65] J. Lu, L. Xu, J. Li, B. Chang, Y. Gui, and H. Liu, *Physics Letters B* **662**, 87 (2008).
- [66] J. Lu, Y. Gui, and L. X. Xu, *European Physical Journal C* **63**, 349 (2009).
- [67] J. Lu, L. Xu, Y. Wu, and M. Liu, *General Relativity and Gravitation* **43**, 819 (2011).
- [68] L. Xu and J. Lu, *JCAP* **2010**, 025 (2010).
- [69] N. Liang, L. Xu, and Z.-H. Zhu, *Astronomy & Astrophysics* **527**, A11 (2011).
- [70] M. Bouhmadi-Lopez, P. Chen, and Y.-W. Liu, *Phys. Rev. D* **84**, 023505 (2011).
- [71] L. Xu, Y. Wang, and H. Noh, *European Physical Journal C* **72**, 1931 (2012).
- [72] R. F. vom Marttens, L. Casarini, W. Zimdahl, W. S. Hipólito-Ricaldi, and D. F. Mota, *Phys. Dark Univ.* **15**, 114 (2017).
- [73] A. Yu. Kamenshchik, U. Moschella, and V. Pasquier, *Phys. Lett.* **B511**, 265 (2001).
- [74] M. C. Bento, O. Bertolami, and A. A. Sen, *Phys. Rev.* **D66**, 043507 (2002).
- [75] V. Gorini, A. Kamenshchik, and U. Moschella, *Phys. Rev. D* **67**, 063509 (2003).
- [76] L. Amendola, F. Finelli, C. Burigana, and D. Carturan, *JCAP* **07**, 005 (2003).
- [77] T. Multamaki, M. Manera, and E. Gaztanaga, *Phys. Rev. D* **69**, 023004 (2004).
- [78] V. Gorini, A. Kamenshchik, U. Moschella, V. Pasquier, and A. Starobinsky, *Phys. Rev. D* **72**, 103518 (2005).
- [79] R. Banerjee, S. Ghosh, and S. Kulkarni, *Phys. Rev. D* **75**, 025008 (2007).
- [80] L. Xu, J. Lu, and Y. Wang, *European Physical Journal*

- C **72**, 1883 (2012).
- [81] J. Lu, D. Geng, L. Xu, Y. Wu, and M. Liu, JHEP **02**, 071 (2015).
- [82] R. Herrera, N. Videla, and M. Olivares, Eur. Phys. J. C **76**, 35 (2016).
- [83] J. Simon, L. Verde, and R. Jimenez, Phys. Rev. D **71**, 123001 (2005).
- [84] D. Stern, R. Jimenez, L. Verde, M. Kamionkowski, and S. A. Stanford, JCAP **02**, 008 (2010).
- [85] C. Zhang, H. Zhang, S. Yuan, S. Liu, T.-J. Zhang, and Y.-C. Sun, Research in Astronomy and Astrophysics **14** (2014).
- [86] A. L. Ratsimbazafy, S. I. Loubser, S. M. Crawford, C. M. Cress, B. A. Bassett, R. C. Nichol, and P. Väisänen, Mon. Not. Roy. Astron. Soc. **467**, 3239 (2017).
- [87] N. Borghi, M. Moresco, and A. Cimatti, Astrophys. J. Lett. **928**, L4 (2022).
- [88] S. Cao and B. Ratra, Phys. Rev. D **107**, 103521 (2023).
- [89] M. Abdul Karim et al. (DESI), Phys. Rev. D **112**, 083515 (2025).
- [90] J. Morawetz et al. (DESI), arXiv:2508.11811 (2025).
- [91] R. R. Caldwell and E. V. Linder, Phys. Rev. Lett. **95**, 141301 (2005).
- [92] R. R. Caldwell, Phys. Lett. **B545**, 23 (2002).
- [93] E. Elizalde, S. Nojiri, and S. D. Odintsov, Phys. Rev. **D70**, 043539 (2004).
- [94] M. Moresco, A. Cimatti, R. Jimenez, L. Pozzetti, G. Zamorani, M. Bolzonella, J. Dunlop, F. Lamareille, M. Mignoli, H. Pearce, et al., JCAP **2012**, 006 (2012).
- [95] M. Moresco, Mon. Not. Roy. Astron. Soc. **450**, L16 (2015).
- [96] M. Moresco, L. Pozzetti, A. Cimatti, R. Jimenez, C. Maraston, L. Verde, D. Thomas, A. Citro, R. Tojeiro, and D. Wilkinson, JCAP **05**, 014 (2016).
- [97] J. Torrado and A. Lewis, JCAP **05**, 057 (2021).
- [98] A. Lewis, JCAP **08**, 025 (2025).
- [99] C. M. Hurvich and C.-L. Tsai Sai, Biometrika **76**, 297 (1989).
- [100] H. Akaike, IEEE Transactions on Automatic Control **19**, 716 (1974).
- [101] G. E. Schwarz, Annals of Statistics **06**, 461 (1978).
- [102] K. P. Burnham and D. R. Anderson, *Model Selection and Multimodel Inference: A Practical Information-Theoretic Approach* (Springer-Verlag, New York, 2002), 2nd ed.
- [103] T. D. Saini, S. Raychaudhury, V. Sahni, and A. A. Starobinsky, Phys. Rev. Lett. **85**, 1162 (2000).